

## Scapolite cell-parameter trends along the solid-solution series

DAVID K. TEERTSTRA AND BARBARA L. SHERRIFF

Department of Geological Sciences, University of Manitoba, Winnipeg, Manitoba R3T 2N2, Canada

### ABSTRACT

Scapolites are tetragonal framework aluminosilicates with the general formula  $M_4T_{12}O_{24}A$ , the major constituents being  $M = Na + Ca$ ,  $T = Si + Al$ , and  $A = Cl + CO_3 + S$ -bearing anions, along with minor Fe, Sr, Ba, K, and H. Substitutions among the M, T, and A sites are independent and constrained only by net charge balance and maximum site occupancy. The cell parameters vary primarily with framework chemistry and Al-Si order and are not a strong function of the M- or A-site substitutions. End-member marialite has  $a = 12.06(1)$  and  $c = 7.551(5)$  Å, and meionite has  $a = 12.20(1)$  and  $c = 7.556(5)$  Å. Changes in cell-parameter trends in the series occur at  $Al_{3.6}Si_{8.4}O_{24}$  and  $Al_{4.7}Si_{7.3}O_{24}$  and are correlated with the locations of  $P4_2/n-I4/m$  phase transitions. The scapolite group can be divided into three isomorphous series:  $9.0 > Si > 8.4$ ,  $8.4 > Si > 7.3$ , and  $7.3 > Si > 6.0$ , each with its own patterns of Al-Si order. Because scapolites with the same Si content have variable cell parameters, there might be variable degrees of Al-Si order or a minor, secondary influence of the M- or A-site substituents.

### INTRODUCTION

Scapolites are framework aluminosilicates with tetragonal symmetry. Scapolite lacks any twinning or exsolution features but displays a wide range of solid solution. Common to many metamorphic terrains, and stable over a wide range of pressures and temperatures, scapolite has potential as a geothermometer and geobarometer (Orville 1975; Goldsmith and Newton 1977; Baker and Newton 1994). Scapolite is unique among rock-forming minerals in that it contains information about the activities of the volatiles  $CO_2$ , Cl,  $SO_3$ , and  $H_2O$ , as well as potential information on Eh (from Fe valence) and pH (from anion speciation). Scapolite may also be found on Mars and is identified in chondritic meteorites (Gooding and Muenow 1986; Alexander et al. 1987; Swayze and Clark 1990).

The general formula is  $M_4T_{12}O_{24}A$ , where the major components are  $M = Na$  and  $Ca$ ,  $T = Si$  and  $Al$ , and  $A = Cl$ ,  $CO_3$ , and S-bearing anions. The minor components are Fe, Sr, Ba, K, and H. The mineral group has only two presently accepted species (Bayliss 1987). The idealized end-member formulae are marialite (Ma)  $Na_4Al_3Si_9O_{24}Cl$  and meionite (Me)  $Ca_4Al_6Si_6O_{24}CO_3$ . The stoichiometry of the Ma-Me solid-solution series may be understood in terms of three independent substitutions: (1) variations in Si/Al ratios of the framework T sites, (2)  $2M^+ = M^{2+}$  substitutions in the interstitial M sites (primarily  $Na^+$  and  $K^+$  for  $Ca^{2+}$ ), and (3)  $2A^- = A^{2-}$  substitutions in the A-anion site (primarily  $Cl^-$  for  $CO_3^{2-}$  and S-bearing anions). The crystal-chemical roles of certain minor elements are poorly understood in terms of assignment of specific species to the formula, e.g., Fe may enter the T or M sites, and H may be present as  $H^+$ ,  $OH^-$ , or  $H_2O$ . There does

not seem to be any simple quantitative substitutional mechanisms between the M, T, and A sites; e.g., scapolites with one Si/Al ratio may range in Me content because of complex coupled substitutions that include the A site. Me may be defined as the percent of divalent cations in the M site [ $Me = 100(\Sigma \text{divalent cations})/4$ ]. The stoichiometry of scapolite is variable but within the limits of net charge balance and maximum site occupancy, and this allows for a wide range of scapolite stability.

One of the main topics of interest in scapolite has been the relationship between composition and change of space group from  $I4/m$  to  $P4_2/n$ . The basic crystal-chemical cause for the structural change has not been clarified (Aitken et al. 1984). Previous workers have plotted cell parameters against Me [ $=100Ca/(Na + Ca + K)$ ] but have not investigated how the resulting trends are related to the M-site substitutions: Because of the uncertain role of Fe and H, the formula of scapolite is more complex than most workers suggest. The cell volume increases from Ma to Me, but because  $Na^+$  and  $Ca^{2+}$  have virtually identical ionic radii, the cause of this increase requires investigation. Furthermore, the previous interest was a change in trend among Ca-rich scapolites; the Na-rich portion of the series has not been systematically examined.

In this study, we examine a set of scapolite samples that have been widely disseminated for scientific study and are commonly used as analytical reference standards because they are well characterized. This allows us to compare data for the same samples from different laboratories. These particular scapolite samples have been examined by a variety of methods, including infrared spectroscopy (IR) (Wehrenberg 1971; Swayze and Clark 1990), carbon isotope measurements (Moecher et al. 1994),

thermal and mass spectrometer analysis (Graziani and Lucchesi 1982), thermal and X-ray analysis (Baker 1994), laser Raman spectroscopy (Donnay et al. 1978), powder X-ray diffraction (XRD) (Haughton 1971; Lin and Burley 1973b; Ulbrich 1973a), nuclear magnetic resonance (NMR) (Sherriff et al. 1987), and transmission electron microscopy (TEM) (Hassan and Buseck 1988). Dielectric constants were determined by Shannon et al. (1992) and compressibility by Hazen and Sharp (1988) and Comodi et al. (1990).

### PREVIOUS WORK

Early studies of cell parameters across the scapolite series were published by Eugster et al. (1962), Lin and Burley (1973b), Ulbrich (1973a), and Haga (1977). There are differences in the interpretation of these data; e.g., for the *c* cell edge vs. Me, conclusions include a constant value, a linear decrease, and a decrease to Me<sub>65</sub> then an increase. Stability relations and phase equilibria were studied by Goldsmith and Newton (1977), Aitken (1983), and Orville (1975), and X-ray analysis of these synthetic scapolites show neither a compositional gap from Ma to Me nor any trend change in cell parameters. However, Baker (1994) examined the Ca-rich portion of the series and documented a change in cell-parameter trends at about Al<sub>3</sub>Si<sub>7</sub>O<sub>24</sub>. Baker reviewed only a fraction of the available literature and calculated the formula on the basis of 16 cations rather than 12 T cations, which is incorrect if there are vacancies in the M site. The trends of cell parameters with composition require careful reexamination.

The thermal expansion of scapolite was studied by Levien and Papike (1976), Graziani and Lucchesi (1982), Baker and Newton (1994), and Baker (1994). No phase transition was found at any temperature. There is an approximately linear increase in the *a* cell edge with temperature as *c* remains constant. This indicates that at room temperature, scapolite is fully expanded along (001).

In contrast to the effects of temperature, both the *a* and *c* cell edges decrease linearly with pressure. The unit-cell compression is essentially isotropic because there is a constant *c*:*a* axial ratio (Hazen and Sharp 1988; Comodi et al. 1990). Comodi et al. (1990) estimated geothermal gradients of 22 °C/km for Na-rich scapolites and 27 °C/km for the more common Ca-rich scapolites, along which the unit-cell parameters are invariant.

Two phase changes have been correlated with Me content. Single-crystal X-ray structure refinements show that intermediate members of the series are in space group  $P4_2/n$  and that the end-members are in  $I4/m$  (Belokoneva et al. 1991, 1993; Comodi et al. 1990; Papike and Zoltai 1965; Lin and Burley 1973a, 1973b, 1975; Levien and Papike 1976; Papike and Stephenson 1966; Aitken et al. 1984; and Ulbrich 1973b). In contrast, TEM examinations of antiphase domains indicate that on this scale the symmetry of the intermediate members may be  $P4/m$  or  $P4$  (Hassan and Buseck 1988; Oterdoom and Wenk 1983). Bulk samples may be considered as a mix of Cl and CO<sub>3</sub> clustered domains within an unchanged

framework; alternatively, the domains may be produced by Al-Si ordering. NMR observations suggest that there are alternating stacks of ordered T sites in the structure (Sherriff et al. 1987). Any model of cation or anion order in scapolites must reconcile these long-range and short-range observations. The space group changes from the intermediate members to the end-members are second-order phase transitions, and XRD should be capable of locating their positions along the series.

The marialite-rich portion of the series has not been extensively examined because natural occurrences are relatively rare. Only recently, Lieftink et al. (1993) reported on the chemistry of Na- and Cl-rich scapolites from Bamble, Norway; however, no X-ray data were presented. With an A site essentially filled with Cl, Lieftink and coworkers found 3.7 atoms of Al per formula unit (pfu) instead of the ideal 3.0. The compositional trends indicate that as Me approaches zero, Si/Al ratios are <3.0, in disagreement with the idealized formula Na<sub>4</sub>Al<sub>3</sub>Si<sub>5</sub>O<sub>24</sub>Cl. In a powder XRD study of Na- and Cl-rich gem scapolites from the eastern Pamirs, Zolotarev (1993) found that cell-edge plots with Me content revealed two changes in trend along the series.

Although the chemical studies indicate at least three potential changes in isomorphic substitutions along the scapolite solid solution, XRD indicates at least two probable trend changes. The position of the compositional changes has not been properly correlated with that of the second-order phase transitions. Here we review the existing information and combine it with new compositional and X-ray powder diffraction data to elucidate relationships between crystal chemistry and cell parameters.

### EXPERIMENTAL METHODS

#### Analysis of samples

Samples used in this study are described in the Appendix. Most of our samples are fine-grained mineral separates or powdered single crystals. Thin sections were prepared of all samples, but because of fine grain size the optic sign could be determined on only two-thirds of them. All these were uniaxial negative with no indication of biaxial behavior, in contrast to the reports of Gouveia and Villarreal (1981).

Compositions were measured using a CAMECA SX-50 electron microprobe operating at 15 kV and 20 nA with a beam diameter of 10 μm. Data were reduced using the PAP procedure of Pouchou and Pichoir (1985). A summary of the analytical conditions is given in Table 1. Our principal reference standards were the following: a gem-quality meionite from Brazil, USNM no. R6600-1 (Dunn et al. 1978); albite from the Amelia County courthouse, Virginia; anorthite from Sitkin Island; and tugtupite from the type locality, south Greenland R.O.M. no. M32790. Our standards cross-analyzed within experimental error. Each sample was checked for homogeneity by analysis. Compositions were determined on the same powders from which the cell parameters were measured.

Analytical accuracy was checked by comparison with results of bulk analysis on the same samples published in the literature.

Absolute quantities of H<sub>2</sub>O were determined at 900 °C in a Karl Fischer titration using a Mitsubishi moisture meter. CO<sub>2</sub> contents were derived from bulk determinations on the samples reported in the literature (Shaw 1960a; Shaw et al. 1965; Evans et al. 1969; Moecher 1988).

XRD data were collected using a Siemens D5000 automated diffractometer operating in transmission geometry. Si (NBS standard reference material 640b) was used as an external standard for calibration before and after data collection. Si was used as an internal standard for one sample, but the contamination had to be avoided for the other samples so that no sample was lost for later studies. Finely ground samples of scapolite were mounted onto 4 μm thick Prolene film using L'Oréal hairspray as a mounting medium. The 20 mg sample quantities were found to give the best peak/background ratios. A Huebner incident-beam monochromator was used to obtain CuKα<sub>1</sub> X-radiation generated using 40 kV and 35 mA with a fine-focus X-ray tube. The sample was rotated 60 rpm during the data collection. A 2 mm antiscatter slit, a 0.6 mm receiving slit, and a Kevex solid-state detector were used. Most of the data were collected from 9 to 49° 2θ using a step width of 0.02° with 5 s counting time per step. These conditions provided sufficient accuracy and precision for the purposes of this study but were improved for several of the samples with longer count times, smaller step widths, and scanning to higher 2θ values. Cell parameters were refined as orthorhombic but were identical, within error, to the tetragonal cells.

### Formula calculations

When dealing with relatively subtle cell-parameter trends associated with composition, the method of formula calculation is important. The general formula M<sub>4</sub>T<sub>12</sub>O<sub>24</sub>A is based on models of the crystal structure in which trivalent and tetravalent cations occupy the tetrahedrally coordinated sites of a TO<sub>2</sub> framework, monovalent and divalent cations occupy the interstitial M sites, and extraframework anions occupy the A-site cavity. Most researchers calculate scapolite formulae by normalization to 12(Si + Al), thereby assuming no T-site vacancy. The formula has also been based on 16 cations, but this is incorrect if there are M-site vacancies. All previous authors have calculated CO<sub>2</sub> contents by assuming that the A site is filled and using the formula C = 1 - Cl - F - S, but this simplistic approach ignores charge-balance considerations and the importance of H. Our method of formula calculation is explained below and representative examples are given.

The formula of scapolite is initially calculated by normalizing to 12 T cations, where T = Si + Al. Monovalent and divalent cations (including Fe) are assigned to the M site. The sum of the M cations should not exceed 4 atoms per formula unit (apfu). Vacancies in the M site are pos-

TABLE 1. Collection of analytical data

Standard	X-ray line	t (s)	Oxide	L.D. (wt%)
Albite	NaKα	20	Na <sub>2</sub> O	0.049
	SiKα	20	SiO <sub>2</sub>	0.060
Anorthite	CaKα	20	CaO	0.025
	AlKα	20	Al <sub>2</sub> O <sub>3</sub>	0.045
Scapolite	AlKα	20	Al <sub>2</sub> O <sub>3</sub>	0.045
Tugtupite	ClKα	20	—	0.014
Anhydrite	SKα	40	SO <sub>3</sub>	0.050
Orthoclase	KKα	20	K <sub>2</sub> O	0.036
Almandine	FeKα	40	Fe <sub>2</sub> O <sub>3</sub>	0.086
SrTiO <sub>3</sub>	SrLα	60	SrO	0.059
	TiKα	80	TiO <sub>2</sub>	0.057
Riebeckite	FKα	120	—	0.069
VP <sub>2</sub> O <sub>7</sub>	PKα	60	P <sub>2</sub> O <sub>5</sub>	0.073
Sanidine	BaLα	80	BaO	0.087
Pyrope	MgKα	80	MgO	0.010
Spessartine	MnKα	120	MnO	0.025
PbTe	PbMα	60	PbO	0.041

Note: Limits of detection were calculated using L.D. =  $\{3(\text{wt}\% \text{ oxide}) (R_b/t_b)^{1/2}\} / (R_p - R_b)$ , where  $R_b$  = background count rate (counts per second),  $t_b$  = background count time (seconds), and  $R_p$  = peak count rate.

sible (M < 4 apfu) and appear to be common in natural scapolite. If M is greater than 4 the excess portion of the Fe<sup>2+</sup> in M is assigned as Fe<sup>3+</sup> in T. The formula is then renormalized to Si + Al + Fe<sup>3+</sup> = 12 and the Σ M recalculated. This is an iterative process from which Fe<sup>2+</sup>/Fe<sup>3+</sup> ratios are obtained. This calculation is a useful means of balancing the formula and is therefore indirect evidence for the substitutions. However, there is no spectroscopic evidence indicating the role of Fe in scapolite, although many wet-chemical determinations report both Fe<sup>2+</sup> and Fe<sup>3+</sup>. We should emphasize that Fe contents are minor, exert only a small influence on T-site or Me contents, and do not significantly affect cell-parameter trends with Si apfu. However, in some cases the assignment of Fe is significant for charge-balance considerations.

The net charge balance is assessed by subtracting the negative charge generated by the framework (TO<sub>4</sub><sup>-</sup>) from the positive charge of the M cations (M<sup>+</sup>). This excess positive charge should equal the charge of the A anions (A<sup>-</sup>) such that M<sup>+</sup> - TO<sub>4</sub><sup>-</sup> = A<sup>-</sup>, where TO<sub>4</sub><sup>-</sup> = Al + Fe<sup>3+</sup> and M<sup>+</sup> = Na + K + 2(Ca + Sr + Ba + Fe<sup>2+</sup>). Note that moving Fe from the M site to the T site doubly reduces the calculated excess positive charge because one positive charge moved from M to T results in a negative charge added to TO<sub>4</sub><sup>-</sup>. It also reduces the number of calculated A-site molecules such that A is no greater than one, again providing a better balanced formula in some cases.

Cl and S contents are usually determined by EMP analysis, and with an assumption of a divalent S species the remaining anion charge may be calculated. This may be assigned to a divalent C species giving a calculated CO<sub>3</sub><sup>2-</sup> pfu. Molecular occupancy of the A site should not exceed 1 pfu; however, as in the M site, vacancy is possible. The existence of a vacancy cannot be determined without measuring all the volatile species, including H<sub>2</sub>O, because of the presence of bicarbonate or bisulfate (Swayze and Clark 1990).

If H<sub>2</sub>O is determined and a positive charge remains,

TABLE 2. Cell parameters of scapolite from the literature

<i>a</i> (Å)	<i>c</i> (Å)	Me (%)	Si (pfu)	Reference	<i>a</i> (Å)	<i>c</i> (Å)	Me (%)	Si (pfu)	Reference
12.197	7.577	90.5	6.35	1	12.189	7.576	92.8	6.26	18
12.143	7.569	59.3	7.43	1	12.064	7.583	32.8	8.08	19
12.073	7.585	34.6	8.00	1	12.054	7.586	33.7	8.02	19
12.063	7.582	21.5	8.28	1	12.081	7.581	39.5	7.95	19
12.047	7.568	9.5	8.78	2	12.111	7.578	47.5	7.75	19
12.042	7.578	17.2	8.56	2	12.142	7.567	58.8	7.46	19
12.039	7.576	11.3	8.72	2	12.165	7.574	79.0	6.84	19
12.048	7.567	9.4	8.78	2	12.067	7.585	32.5	8.09	19
12.048	7.566	6.9	8.85	2	12.090	7.581	36.6	7.96	19
12.051	7.561	5.6	8.94	2	12.118	7.576	48.0	7.61	19
12.064	7.584	31.4	8.18	2	12.121	7.572	49.6	7.64	19
12.073	7.587	34.0	8.06	2	12.145	7.576	66.1	7.28	19
12.069	7.582	26.5	8.18	3	12.148	7.565	67.5	7.21	19
12.014	7.597	17.0	8.47	4	12.150	7.564	68.3	7.18	19
12.191	7.575	87.3	6.47	5	12.150	7.563	69.5	7.14	19
12.179	7.571	84.9	6.58	6	12.151	7.564	70.5	7.13	19
12.192	7.575	85.2	6.47	7	12.156	7.564	71.2	7.11	19
12.200	7.578	90.9	6.29	7	12.160	7.565	72.1	7.03	19
12.014	7.597	17.0	8.47	8	12.201	7.579	92.8	6.26	19
12.045	7.587	28.0	8.10	8	12.046	7.599	49.5	7.97	20
12.083	7.583	38.5	7.80	8	12.060	7.577	18.9	8.33	21
12.087	7.577	42.8	7.76	8	12.075	7.580	33.0	8.04	21
12.134	7.571	52.6	7.59	8	12.068	7.577	40.2	7.91	21
12.147	7.566	58.6	7.47	8	12.057	7.579	42.9	7.81	21
12.147	7.562	67.1	7.30	8	12.090	7.579	43.8	7.85	21
12.185	7.578	85.3	6.32	8	12.087	7.584	45.8	7.94	21
12.163	7.578	78.2	6.99	9	12.095	7.579	46.3	7.80	21
12.168	7.573	74.9	6.97	9	12.099	7.579	46.1	7.76	21
12.158	7.569	73.9	7.04	9	12.113	7.576	51.5	7.61	21
12.158	7.573	75.3	7.10	10	12.135	7.588	58.6	7.44	21
12.043	7.560	10.4	8.70	11	12.142	7.566	64.5	7.19	21
12.059	7.583	20.7	8.27	12	12.154	7.575	77.7	6.79	21
12.037	7.566	15.4	8.55	13	12.071	7.589	32.5	7.97	22
12.058	7.586	25.4	8.32	14	12.070	7.586	38.5	7.94	23
12.069	7.581	33.0	8.04	15	12.169	7.569	66.9	6.96	24
12.086	7.578	43.5	7.69	16	12.142	7.576	65.0	7.24	24
12.059	7.587	18.9	8.33	17	12.106	7.577	46.9	7.73	24
12.060	7.589	32.2	8.05	17	12.095	7.579	46.1	7.80	24
12.071	7.582	33.0	8.04	17	12.075	7.580	33.0	8.04	24
12.063	7.585	39.5	7.95	17	12.060	7.577	18.9	8.33	24
12.156	7.556	66.9	6.96	17	12.095	7.571	53.1	7.64	25
12.147	7.576	65.0	7.24	17	12.163	7.569	67.2	6.78	25
12.168	7.571	77.7	6.79	17	12.137	7.561	68.4	7.08	26
12.194	7.557	92.8	6.26	17	12.090	7.580	45.8	7.78	27

Note: 1 = Baker (1994), 2 = Zolotarev (1993), 3 = Shannon et al. (1992), 4 = Comodi et al. (1990), 5 = Hazen and Sharp (1988), 6 = Aitken et al. (1984), 7 = Oterdoom and Wenk (1983), 8 = Graziani and Lucchesi (1982), 9 = Boivin and Camus (1981), 10 = Peterson et al. (1979), 11 = Zwaan (1979), 12 = Llambias et al. (1977), 13 = Strunz and Wilk (1976), 14 = Smetzer et al. (1976), 15 = Levien and Papike (1976), 16 = Orville (1975), 17 = Lin and Burley (1973b), 18 = Ulbrich (1973a), 19 = Ulbrich (1973b), 20 = El Shazly and Saleeb (1972), 21 = Haughton (1971), 22 = Mykura and Young (1969), 23 = Kuznetsova and Skarzynsky (1968), 24 = Papike (1964), 25 = Gibbs and Bloss (1961), 26 = Marchenko (1961), and 27 = Schiebold and Seumel (1932).

enough may be assigned as OH<sup>-</sup> to balance charges. If there is a net negative charge, this may be assigned as H<sup>+</sup>. With a zero net charge, the remainder might be molecular H<sub>2</sub>O.

There is a significant role for H in scapolite: Only one of the 20 scapolites examined in this study was anhydrous. Donnay et al. (1978) used laser Raman spectroscopy to demonstrate the presence of HCl, whereas Swayze and Clark (1990) used IR spectroscopy to measure bicarbonate and bisulfate. Additional species such as H<sub>2</sub>O, OH<sup>-</sup>, HS<sup>-</sup>, HSO<sub>3</sub><sup>-</sup>, and H<sub>2</sub>S are possible. The speciation of the A-site anions cannot be determined by formula calculations because spectroscopic measurements are necessary to determine the proportion of species in the equilibrium HCl + CO<sub>3</sub><sup>2-</sup> = Cl<sup>-</sup> + HCO<sub>3</sub><sup>-</sup>. If all C is in the form of CO<sub>3</sub><sup>2-</sup>, there may be an apparent vacancy; in contrast, the A site may be filled if a fraction is in the

form of HCO<sub>3</sub><sup>-</sup>. As an example, consider an F- and S-free scapolite with an excess positive charge of M<sup>+</sup> - TO<sub>4</sub><sup>-</sup> = +0.94 and Cl = 0.44 apfu. Subtracting Cl<sup>-</sup> from the excess positive charge gives +0.50 pfu. If this is charge balanced by CO<sub>3</sub><sup>2-</sup>, then 0.25 molecules are required and Σ A = 0.69 pfu; however, if it is balanced by 0.50 HCO<sub>3</sub><sup>-</sup> molecules, then Σ A = 0.94 pfu.

## RESULTS AND DISCUSSION

Cell-parameter and compositional data for natural scapolites quoted in the literature are given in Table 2. Unit-cell formulae were calculated by the method described above. This method is an improvement over previous methods because it accounts for both charge-balance considerations and maximum site occupancy. Results of chemical analysis and tetragonal cell-parameter refine-

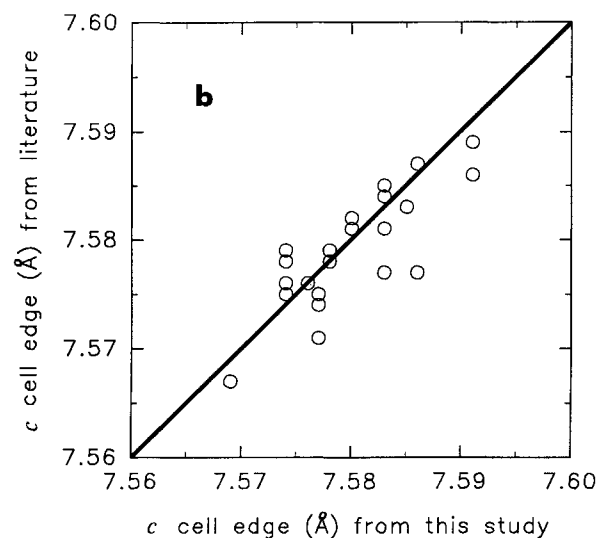
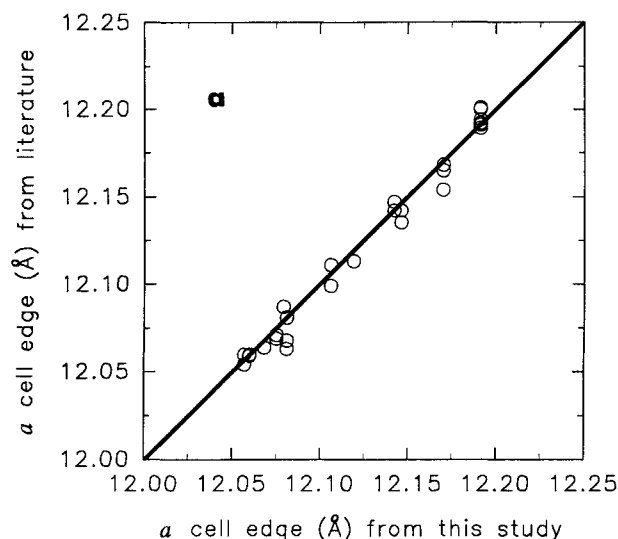


FIGURE 1. Plots of (a)  $a$  cell edges and (b)  $c$  cell edges reported in the literature vs. our measurements on the same sample. Note the change in scale from a to b.

ments for our samples are given in Table 3. Ti, P, Mg, Mn, and Pb were not detected in any of the samples. Representative results of the formula calculations are given in Table 4. Over a range of Me content, these results give examples of the Fe valence calculations, indicate up to 19% vacancy in the M site (ON8), and indicate H- and OH-rich scapolites.

The X-ray data were checked for error by plotting the cell parameters determined in this study against published results for the same samples (Figs. 1a and 1b). The between-lab variance is estimated to be  $\pm 0.01$  Å in  $a$  and  $\pm 0.005$  Å in  $c$ . The minimum precision of our refinements was  $\pm 0.003$  Å in  $a$  and  $\pm 0.002$  Å in  $c$ .

Plots of  $a$  vs.  $c$  and  $a$  vs.  $V$  were prepared to demonstrate that changes in cell-parameter trends are not arti-

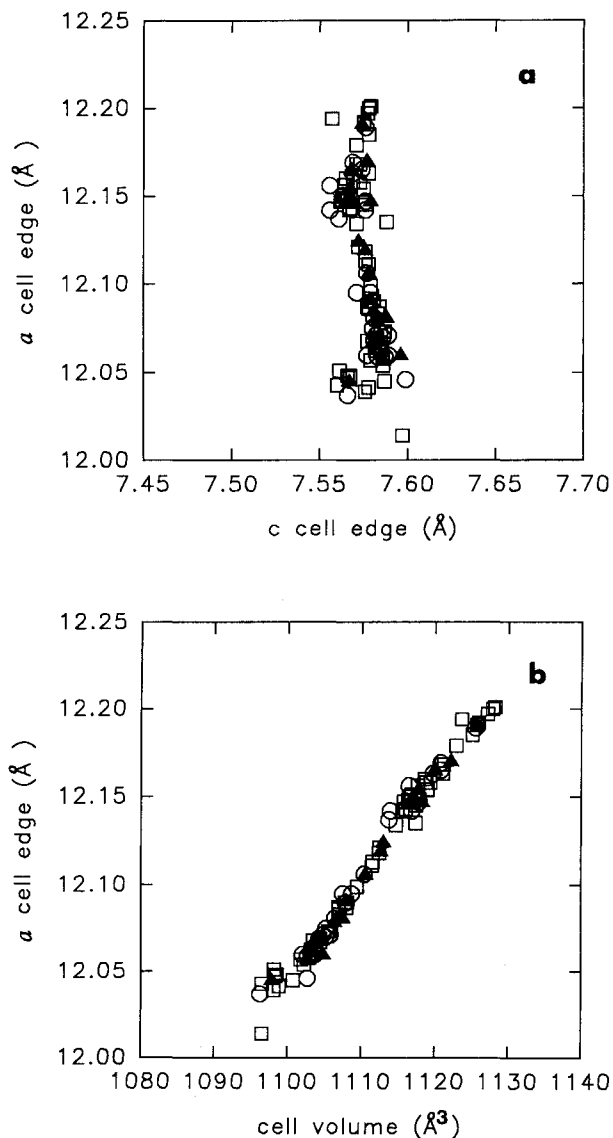


FIGURE 2. (a) Cell-parameter trends of  $a$  vs.  $c$ , and (b) cell edge  $a$  vs. cell volume,  $V$ . Symbols are for data from this study (triangles) and from the literature, including compositions determined by bulk wet-chemical methods (circles) and EMP analysis (squares).

facts of the method of formula calculation or linked to changes in chemical substitutions (Figs. 2a and 2b). The data plotted are from the literature and from this study. Three possible trends in the series are revealed. To understand the cause of the changes in trend, however, the physical data of the cell parameters must be correlated with the chemical data. Information about the crystal structure provides mechanisms linking changes in cell parameters with changes in crystal chemistry.

#### Structural role of A-site anions

A survey of the literature reveals that surprisingly few scapolites have been analyzed for both  $\text{CO}_2$  and  $\text{H}_2\text{O}$ . In part this is because of the difficulties of preparing a clean

TABLE 3. Analytical results

Oxide (wt%)	PAM	ON8	TANZ	ON7	CA63A	SANT	GL	ON70	MAD	Q26
SiO <sub>2</sub>	61.32	57.58	55.15	54.69	53.88	53.57	54.15	52.53	51.48	51.05
Al <sub>2</sub> O <sub>3</sub>	18.57	21.29	21.96	22.62	22.81	22.69	23.16	23.35	23.90	23.88
Fe <sub>2</sub> O <sub>3</sub>	0.11	0.03	0.12	0.00	0.11	0.10	0.01	0.10	0.07	0.11
Na <sub>2</sub> O	13.20	11.37	9.17	8.91	8.26	8.20	8.89	7.38	6.86	5.98
K <sub>2</sub> O	0.75	0.65	1.33	0.92	1.42	1.15	0.16	1.14	0.50	1.05
CaO	1.23	3.07	6.94	7.77	8.32	8.57	8.92	9.96	11.34	11.97
SrO	0.06	0.02	0.07	0.10	0.28	0.09	0.13	0.07	0.10	0.20
BaO	0.04	0.08	0.03	0.04	0.02	0.00	0.14	0.00	0.04	0.00
Cl	3.96	2.15	2.99	2.90	2.75	2.84	2.45	1.94	1.84	1.69
F	0.00	0.04	0.03	0.00	0.15	0.00	0.03	0.06	0.05	0.00
SO <sub>3</sub>	0.13	0.01	0.86	0.00	0.17	0.45	0.16	1.48	0.81	1.24
CO <sub>2</sub>	—	1.11	1.14	1.50	—	—	1.90	2.18	2.28	2.55
H <sub>2</sub> O	—	0.44	0.14	0.32	0.20	0.00	0.35	0.11	0.14	0.22
Sum	99.37	97.85	99.93	99.77	98.38	97.66	100.45	100.30	99.41	99.94
O = Cl, F	-0.89	-0.50	-0.69	-0.67	-0.68	-0.64	-0.57	-0.46	-0.43	-0.38
Total	98.48	97.35	99.24	99.10	97.70	97.02	99.88	99.84	98.98	99.56
Si/Al	8.84	8.36	8.17	8.07	8.01	8.01	7.98	7.88	7.76	7.74
Me (%)	4.9	12.2	27.9	30.8	33.6	34.8	35.5	40.4	46.1	49.0
a (Å)	12.045	12.060	12.067	12.068	12.079	12.081	12.057	12.081	12.091	12.106
c (Å)	7.567	7.596	7.580	7.585	7.583	7.588	7.586	7.583	7.579	7.578

bulk separate (as documented in sample descriptions). Therefore, it is difficult to make an overall assessment of the speciation and stoichiometry of the A site. Plots of cell parameters against A-site chemistry are highly scattered because of the poorly defined role of volatiles in scapolite. Nevertheless, several lines of evidence indicate the structural influence of A-site anions on the cell parameters.

The unit-cell parameters of scapolite are completely reversible on heating up to 800 °C, despite the loss of H<sub>2</sub>O at 200–400 °C, SO<sub>2</sub> at 300–600 °C, and CO<sub>2</sub> at 400–800 °C (Graziani and Lucchesi 1982). Beyond about 800 °C, NaCl and KCl are volatilized, and on cooling the cell parameters remain permanently increased. A comparison of the heating experiments of Baker (1994) in an N<sub>2</sub> atmosphere with those of Graziani and Lucchesi (1982) in an O<sub>2</sub> atmosphere indicates that volatile loss is accentuated in O<sub>2</sub> relative to N<sub>2</sub>. This may be due to anion sub-

stitutions such as O<sup>2-</sup> = CO<sub>3</sub><sup>2-</sup> (Aitken et al. 1984). Levien and Papike (1976) concluded that the main cause of permanently increased cell parameters on heating above 800 °C is Al-Si disorder because their heating experiments in a sealed vessel indicated no loss of volatiles.

Refinements of the crystal structure show an anion-site volume ( $V_A$ ) that is considerably larger than that of any available anion: for Me-14  $V_A = 94 \text{ \AA}^3$ , for Me-86  $V_A = 103 \text{ \AA}^3$  (see Comodi et al. 1990 for site diameters and diagrams of the structure). The anion cage is a rigid element of the framework structure, and its volume is virtually constant with compression (Comodi et al. 1990). There seems to be no basis for the use of variable S:C ratios to estimate pressure of crystallization (Peterson et al. 1979); we suggest instead that the anion chemistry is solely indicative of volatile activities in the geologic environment.

TABLE 4. Representative results of formula calculations

	PAM	ON8	SANT	MIN	BA15	M18-20-2	MONT
Si	8.835	8.358	8.005	7.466	7.341	7.089	6.165
Al	3.153	3.642	3.995	4.534	4.659	4.911	5.822
Fe <sup>3+</sup>	0.012	0.000	0.000	0.000	0.000	0.000	0.013
Na	3.688	3.200	2.377	1.528	1.515	0.943	0.113
K	0.137	0.120	0.219	0.140	0.092	0.038	0.034
Ca	0.190	0.477	1.372	2.241	2.366	2.955	3.848
Fe <sup>2+</sup>	0.000	0.003	0.011	0.004	0.003	0.007	0.000
Sr	0.001	0.000	0.001	0.004	0.005	0.003	0.001
Ba	0.002	0.005	0.000	0.001	0.000	0.001	0.002
Cl	0.967	0.529	0.720	0.284	0.258	0.024	0.011
F	0.000	0.018	0.000	0.067	0.000	0.000	0.010
S	0.014	0.001	0.051	0.161	0.192	0.003	0.029
C	—	0.220	—	0.570	—	—	0.921
H <sup>+</sup>	—	0.333	0.000	0.018	0.000	0.000	0.000
OH <sup>-</sup>	—	0.000	0.000	0.000	0.182	0.746	0.112
H <sub>2</sub> O	—	0.046	0.000	0.001	0.000	0.000	0.049
M	4.020	3.809	3.980	3.918	3.982	3.949	4.007
A	0.980	0.815	0.771	1.085	0.631	0.772	1.131
Calc. A <sup>-</sup>	1.049	0.656	1.368	1.635	1.697	2.006	2.033
Si/(Al + Fe <sup>3+</sup> )	2.79	2.30	2.00	1.65	1.58	1.44	1.06
Me	4.9	12.2	34.6	56.3	59.4	74.2	96.5

TABLE 3.—Continued

Oxide (wt%)	Q13A	MIN	ON27	BA15	BL136	M-18 20-1	M-18 20-2	BOLT	ON47	MONT
SiO <sub>2</sub>	49.17	48.98	48.66	47.39	46.84	46.60	45.28	46.01	43.20	39.31
Al <sub>2</sub> O <sub>3</sub>	24.96	25.24	25.36	25.52	25.41	25.58	26.62	27.07	27.69	31.50
Fe <sub>2</sub> O <sub>3</sub>	0.04	0.04	0.24	0.02	0.00	0.00	0.07	0.04	0.02	0.11
Na <sub>2</sub> O	5.58	5.17	4.68	5.05	3.74	4.18	3.11	3.90	2.52	0.37
K <sub>2</sub> O	0.72	0.72	1.10	0.47	0.38	0.39	0.19	0.17	0.17	0.17
CaO	12.99	13.72	14.48	14.26	16.50	15.95	17.62	16.72	18.84	22.90
SrO	0.23	0.29	0.11	0.35	0.06	0.12	0.22	0.04	0.20	0.05
BaO	0.08	0.02	0.04	0.00	0.00	0.13	0.02	0.04	0.00	0.00
Cl	1.44	1.10	1.09	0.98	0.31	0.40	0.09	0.52	0.06	0.03
F	0.14	0.14	0.14	0.00	0.03	0.04	0.00	0.11	0.16	0.02
SO <sub>3</sub>	1.26	1.41	0.02	1.65	1.70	1.67	0.03	0.00	2.30	0.25
CO <sub>2</sub>	3.04	2.74	—	—	—	—	—	4.20	3.20	4.30
H <sub>2</sub> O	0.23	0.18	—	0.18	0.90	0.80	0.71	—	0.26	0.20
Sum	99.88	99.75	95.92	95.87	95.87	95.86	93.96	98.84	98.62	99.25
O = Cl, F	-0.39	-0.31	-0.31	-0.22	-0.08	-0.11	-0.02	-0.16	-0.08	-0.01
Total	99.49	99.44	95.61	95.65	95.79	95.75	93.94	98.68	98.54	99.24
Si/Al	7.51	7.47	7.43	7.34	7.32	7.29	7.09	7.09	6.84	6.17
Me (%)	53.5	56.3	60.0	59.4	69.3	67.1	74.2	69.2	79.9	96.5
a (Å)	12.119	12.124	12.146	12.147	12.150	12.146	12.165	12.154	12.170	12.191
c (Å)	7.576	7.572	7.569	7.579	7.567	7.570	7.568	7.567	7.577	7.574

The carbonate group lies strictly within the (001) plane but is disordered over several positions in the anion site. This disorder preserves long-range tetragonal symmetry for the trigonal carbonate group (Aitken et al. 1984). Because of the carbonate disorder there is no long-range distortion of the framework in any one crystallographic direction that could influence a cell parameter, as was suggested by Lin and Burley (1975).

S is a major component in scapolite and can occupy more than 50% of the A site. The dominant S species is probably sulfate with minor bisulfate (Chappell and White 1968; Swayze and Clarke 1990), but there are other possibilities for the speciation of S in the A site. In natural scapolite, IR measurements identify sulfite but cannot distinguish sulfate because of an Si-O absorption overlap (Schwarcz and Speelman 1965). Possibly, a major S species is SO<sub>3</sub><sup>2-</sup> rather than SO<sub>4</sub><sup>2-</sup>, and sulfite might not change the cell parameters like sulfate does as it substitutes for carbonate. A yellow luminescence is due to the presence of S<sub>2</sub><sup>-</sup> (Burgner et al. 1978). HS<sup>-</sup> is also a possible ion because scapolites are H rich. The odor of H<sub>2</sub>S (or CS<sub>2</sub>) was noted on grinding by Ingamells and Gittins (1967), who suggested that these may also be present.

More than one-half of the A site of natural scapolite may be filled by S. In XRD studies of synthetic sulfate scapolite, the *a* cell edge of CO<sub>3</sub> scapolite is about 0.02 Å larger than that of SO<sub>4</sub> scapolite of the same Si/Al ratio (Goldsmith and Newton 1977). Therefore, if S contents of natural scapolite of the same Si/Al ratio are plotted against the *a* cell edge, a trend with a negative slope is expected. In Figure 3a, in which different symbols are used for narrow ranges of Si/Al, a negative slope is not observed. A vertical trend in this plot of S apfu vs. *a* (in angstroms) indicates that the S substitution is independent of the cell edge. Considering the between-laboratory error of ±0.01 Å in *a*, it is possible that the degree of S substitution is not large enough in the samples examined to produce a distinct trend in cell parameters. Neverthe-

less, we did not find any simple relationship between S content and cell dimensions that would overwhelm all other variables.

#### Structural role of M-site cations

In contrast to the A-site volatiles, the M site is chemically well characterized. All the possible constituents are

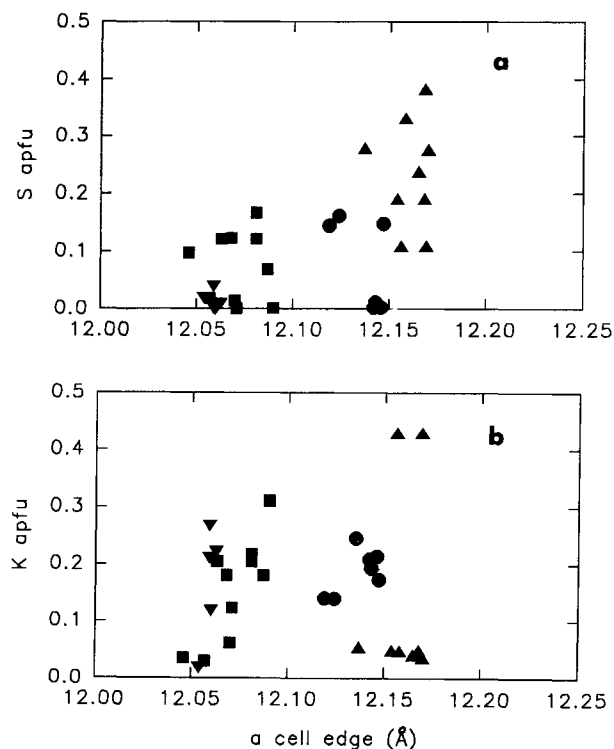
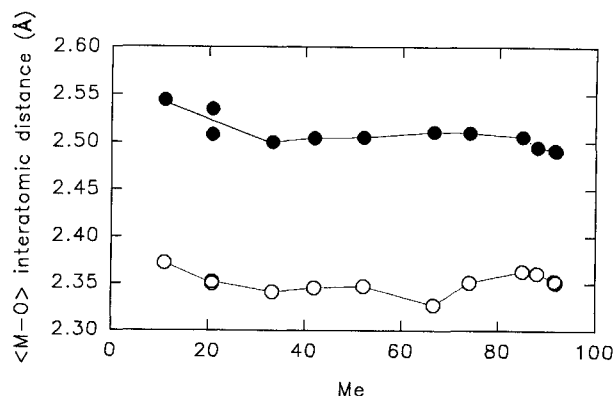


FIGURE 3. Plots of (a) S atoms per formula unit (apfu) vs. *a* cell edge and (b) K apfu vs. *a* cell edge. Data are sorted into the ranges 1.31 < Si/Al < 1.40 (inverted triangles), 1.61 < Si/Al < 1.70 (circles), 1.91 < Si/Al < 2.00 (squares), and 2.21 < Si/Al < 2.30 (triangles).



**FIGURE 4.** Plot of  $\langle M-O \rangle$  interatomic distances vs. Me content  $[=100(\text{divalent cations})/4]$  for  $\langle M-O_2 \rangle$  (open circles) and  $(\langle M-O_3 \rangle + \langle M-O_4 \rangle)/2$  (solid circles). Data are from Belokoneva et al. (1991, 1993), Comodi et al. (1990), Papike and Zoltai (1965), Lin and Burley (1973a, 1973b, 1975), Levien and Papike (1976), Peterson et al. (1979), Papike and Stephenson (1966), Aitken et al. (1984), and Ulbrich (1973b).

usually analyzed, with minimal experimental difficulties, in both wet-chemical and EMP methods. Plots of M-site chemistry against cell parameters are relatively well constrained (e.g., Ulbrich 1973a; Haga 1977) and have been used to estimate Me content. However, because the Pauling ionic radius of  $\text{Ca}^{2+}$  (1.06 Å) is only slightly larger than that of  $\text{Na}^+$  (0.96 Å), any major increase in cell parameters across the series is unlikely to be caused by this substitution.

The M cations are in an irregular, eightfold-coordinated cavity with one bond to an A-site anion and seven bonds to framework O atoms ( $O_2$ ,  $O_3$ ,  $O_4$ ,  $O_5$ ,  $O'_5$ ,  $O_6$ , and  $O'_6$ ). The  $O_2$ ,  $O_3$ , and  $O_4$  atoms have the closest, strongest bonds to the M cation. The interatomic distances of  $\langle M-O_3 \rangle$  and  $\langle M-O_4 \rangle$  are equal. The  $O_5$  atoms are only weakly bonded to the M cation, and similarly the  $O_6$  atoms are too far away to be considered as bonding. A plot of the mean  $\langle M-O \rangle$  interatomic distances against Me shows that these are constant across the series for the three short, strong bonds (Fig. 4). The increase in average bond strength (=cation valence/coordination number) as Ca replaces Na may keep the three closest O atoms at a fixed distance. The correlation of cell parameters with Me seems to be a secondary effect of the Ca-Na substitution because it follows the Al-Si substitution of the framework. Therefore, plots against Me are not advised in the absence of a quantitative description of the substitutional mechanism linking the framework chemistry to that of the M site.

Refinements of the crystal structure indicate that the framework does not have to expand to accommodate Na or Ca (e.g., Belokoneva et al. 1991, 1993). In fact, the site may be slightly too large for Na and Ca. Shannon et al. (1992) accounts for the high polarizability of scapolite by suggesting that cation "rattling" is caused by an oversized M site. The site size is probably determined by the framework, independent of the identity of the M cation.

Me increases with metamorphic grade, and typical samples of high-pressure scapolite are Ca rich. With increasing pressure, cooperative rotation of the four-membered rings of the framework reduces the cross section of the (001) channels along which the M sites are located (Comodi et al. 1990). Both the  $a$  and  $c$  cell edges decrease with increasing pressure. Na-bearing aluminosilicates are usually more compressible than their Ca analogs. Na-O bonds are more compressible than Ca-O bonds, thus the M-site volume decrease is greater and more anisotropic in Na-rich scapolites than in Ca-rich scapolites (Comodi et al. 1990).

The channels expand with increasing temperature, but in contrast to the effects of pressure there is a different sense of rotation of  $T_1$  and  $T_2$  four-membered rings that increases  $a$  without increasing  $c$  (Levien and Papike 1976). An expanded channel could possibly allow substitution of cations larger than Na or Ca.

K is a minor but important constituent of scapolite and has an ionic radius of 1.33 Å, which is large in comparison with that of Na or Ca. Under high- $T$  low- $P$  conditions, scapolites are potentially K-rich if the M site has increased volume. There is no K analog of scapolite, and no XRD data exist for the K-richest scapolites such as those quoted in Shaw (1960a). The substitution of K is apparently limited to about 10–12% (cf. Zolotarev, 1993, and Fig. 3b) by the maximum expansion of the M site. A plot of K apfu vs.  $a$  cell edge should reveal a trend with positive slope if K substitution increases  $a$  cell edge, but this is not observed (Fig. 3b).

#### Structural role of T-site cations

Structurally, scapolites are analogous to zeolites in that they are hydrous framework aluminosilicates with relatively large channels and cavities. In zeolites, the cell parameters vary most closely with changes in the framework composition; the M cations are exchangeable to a degree, and in general their identity does not greatly influence the cell parameters, as we have shown for scapolite. In scapolite, there seems to be minimal influence of the anion chemistry on the unit-cell parameters. Now we turn our attention to the substitutions among tetrahedral framework sites.

The cell parameters  $a$ ,  $c$ , and  $V$  are plotted against Si contents of the framework in Figures 5a, 5b, and 5c, respectively. Si varies from 9.0 apfu ( $\text{Al}_6\text{Si}_9\text{O}_{24}^{3-}$  stoichiometry) at the Na-rich end of the series to 6.0 apfu ( $\text{Al}_6\text{Si}_6\text{O}_{24}^{3-}$ ) at the Ca-rich end of the series. Cell parameter trends extrapolated to Si = 9.0 and Si = 6.0 from Figure 5 indicate that end-member marialite has  $a = 12.06(1)$  and  $c = 7.551(5)$  Å, and end-member meionite has  $a = 12.20(1)$  and  $c = 7.556(5)$  Å.

Over the range  $9.0 > \text{Si} > 8.4$ , decreases in  $a$  are matched by increases in  $c$  such that cell volumes remain relatively constant at about  $1098(1)$  Å<sup>3</sup>. Over the range  $8.4 > \text{Si}/\text{Al} > 6.0$ , cell-volume increases are relatively constant but with a change in trend near Si = 7.4 apfu. Two major changes in trend, marked by arrows in Figure

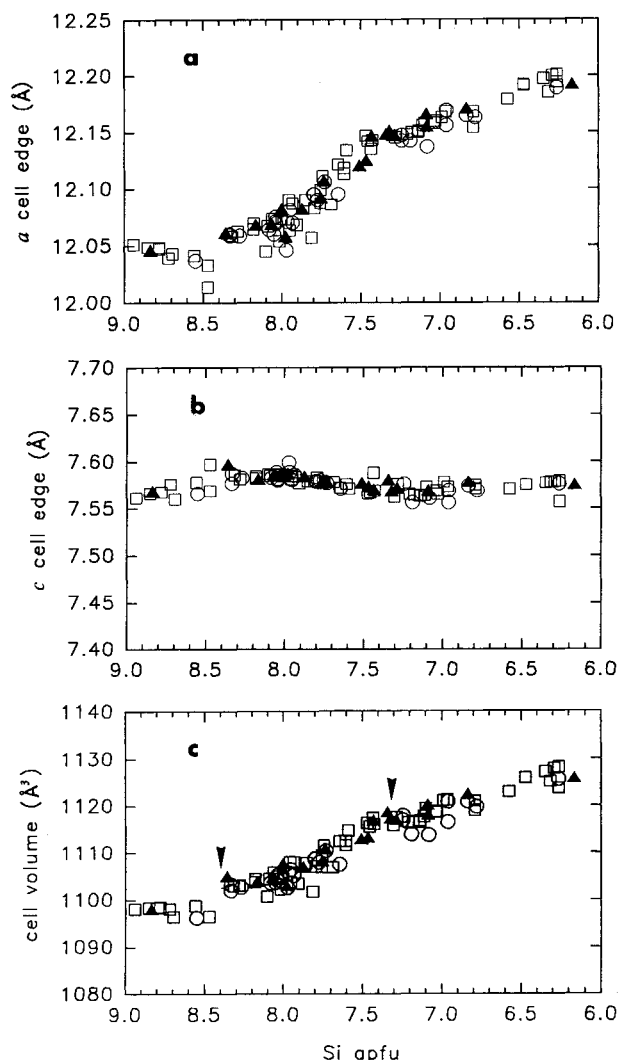


FIGURE 5. Plots of (a)  $a$  cell edge, (b)  $c$  cell edge, and (c) cell volume,  $V$ , vs. Si apfu. Symbols as in Figure 2. Changes in trend at Si = 8.4 and 7.3 are marked by arrows.

5, were located at Si = 8.4 apfu ( $\text{Al}_{3.6}\text{Si}_{8.4}\text{O}_{24}$ ) and 7.3 apfu ( $\text{Al}_{4.7}\text{Si}_{7.3}\text{O}_{24}$ ).

The close correlation of XRD data with T-site chemical data demonstrates that the overall changes in cell parameters across the scapolite series primarily result from the substitution of Al for Si, rather than Na + K for Ca. This approach accurately locates trend changes in the series as a function of composition but does not provide an explanation for them. Single-crystal X-ray diffraction data indicate that trend changes might be related to phase transitions from  $P4_2/n$  in intermediate members of the series to  $I4/m$  in the end-members.

Variations in the average (T-O) interatomic distances are plotted against Si apfu for the three distinct T sites of space group  $P4_2/n$  (Fig. 6). All previous workers plotted data related to the framework against unrelated parameters such as Me% (e.g., Lin 1975; Haga 1977; Oterdoom

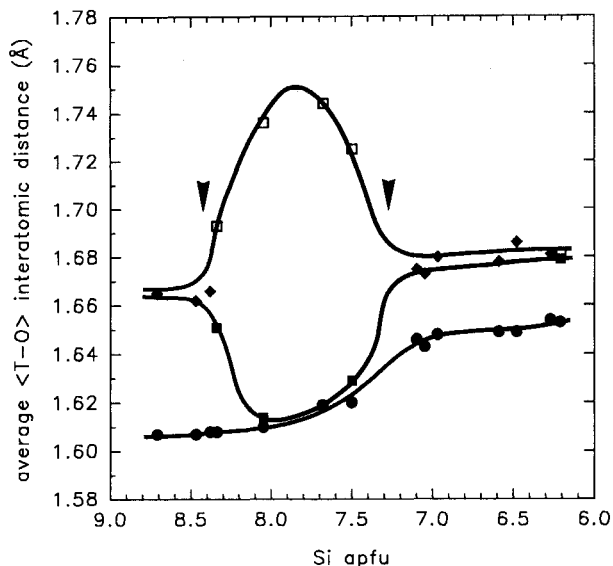


FIGURE 6. Plot of average (T-O) interatomic distances as a function of Si apfu. Midway in the series X-ray structure refinements distinguish three T sites:  $T_1$  (circles),  $T_2$  (open squares), and  $T_3$  (solid squares). Toward each end-member there are only two unique T sites:  $T_1$  and  $T_2 = T_3$  (diamonds). The points of change from three T sites to two are marked by arrows. Data sources are the same as in Figure 4.

and Wenk 1983). From Figure 6 we interpret a highly ordered Al-Si distribution in T sites near  $\text{Al}_{4.2}\text{Si}_{7.8}\text{O}_{24}$  (in contrast to the typically quoted  $\text{Al}_4\text{Si}_8\text{O}_{24}$ ). Here, the  $\langle T_1\text{-O} \rangle$  and  $\langle T_3\text{-O} \rangle$  interatomic distances each equal about 1.61 Å, which is typical for a tetrahedron that is essentially filled with Si. The  $\langle T_2\text{-O} \rangle$  distance attains a maximum of 1.75 Å, which is typical for a site that contains only Al. Toward meionite with Si = 6.0, Al begins to enter the  $T_1$  site, as indicated by increasing  $\langle T_1\text{-O} \rangle$  distances. The changes of long-range symmetry from  $P4_2/n$  to  $I4/m$ , indicated by merging values of  $\langle T_2\text{-O} \rangle$  and  $\langle T_3\text{-O} \rangle$ , occur at about  $\text{Al}_{3.6}\text{Si}_{8.4}\text{O}_{24}$  and  $\text{Al}_{4.7}\text{Si}_{7.3}\text{O}_{24}$ . These are coincident with the locations of the changes in trend of cell parameters.

The above bond-length arguments indicate that cell volumes across the series should increase constantly with the 1:1 substitution of Al for Si; however, they do not. The changes in trend may be related to the patterns of Al-Si order in the structure. The symmetry transitions have been interpreted as a progression from complete order midrange in the series to complete disorder in either end-member (e.g., Lin and Burley 1973a, 1973b, 1975). In contrast,  $^{29}\text{Si}$  and  $^{27}\text{Al}$  NMR data document Al-Si order in the T sites across the series and indicate a continuation of order from midseries toward end-members, with both marialite and meionite being differently but still highly ordered. This dilemma may be solved by the existence of alternating stacks of ordered  $T_2$ - $T_3$  sites throughout the structure (Sherriff et al. 1987). In this case, X-ray structure refinements show apparent disorder be-

cause the alternating stacks are averaged in a long-range experiment. The T sites still contain equal proportions of Si and Al, but the mean  $\langle T_2-O \rangle$  and  $\langle T_3-O \rangle$  distances merge to single values near the changes in trend located by XRD.

Data on cell parameters have clarified this situation because the changes in cell-parameter trends are identified as being coincident with the points of symmetry change. The scapolite group can be divided into three isomorphous series:  $9.0 > Si > 8.4$ ,  $8.4 > Si > 7.3$ , and  $7.3 > Si > 6.0$ . Each series must have its own dominant pattern of Al-Si order. Al-O-Al bonds are probably avoided in Si-rich marialite (Loewenstein 1954); however, because of the presence of five-membered rings in the structure, there must be Al-O-Al bonds in Al-rich meionite (these arguments are summarized in Oterdoom and Wenk 1983). These bonds are probably stabilized by local coordination of the underbonded O atom to Ca (Tossell 1993). Midrange in the series, X-ray structure refinements indicate a well-ordered Al-Si distribution (Lin 1975). The specific patterns of order in the end-members, and the resulting short-range and long-range symmetry, remain to be solved.

For samples of scapolite with the same Si content, the range in cell parameters is up to  $0.03 \text{ \AA}$  in  $a$  and  $0.02 \text{ \AA}$  in  $c$  (this range is ten times our experimental precision). This might be due to a mixture of ordering states, thereby explaining the antiphase domains observed by TEM, or it may be explained by variable Al-Si order. At present we cannot confidently determine whether this range in cell parameters is caused by A- or M-site substitutions or by variable degrees of T-site order within one of the three dominant patterns of order.

#### ACKNOWLEDGMENTS

Samples were kindly provided by D.M. Shaw, B.E. Evans, D.P. Moecher, and A.A. Zolotarev. Laboratory work was funded by NSERC operating grants to B.L.S. A University of Manitoba Duff Roblin Fellowship supported D.K.T. Editorial comments were provided by J. Morrison and the manuscript was improved on the suggestions of an anonymous reviewer.

#### REFERENCES CITED

- Aitken, B.G. (1983)  $T-X_{CO_2}$  stability relations and phase equilibria of a calcic carbonate scapolite. *Geochimica et Cosmochimica Acta*, 47, 351-362.
- Aitken, B.G., Evans, H.T., Jr., and Konnert, J.A. (1984) The crystal structure of a synthetic meionite. *Neues Jahrbuch für Mineralogie Abhandlungen*, 149, 309-342.
- Alexander, C.M.O., Hutchinson, R., Graham, A.L., and Yabuki, H. (1987) Discovery of scapolite in the Bishunpur (LL3) chondritic meteorite. *Mineralogical Magazine*, 51, 733-755.
- Baker, J. (1994) Thermal expansion of scapolite. *American Mineralogist*, 79, 878-884.
- Baker, J., and Newton, R.C. (1994) Standard thermodynamic properties of meionite,  $Ca_2Al_6Si_6O_{24}CO_3$ , from experimental phase equilibrium data. *American Mineralogist*, 79, 478-484.
- Bayliss, P. (1987) Mineral nomenclature: Scapolite. *Mineralogical Magazine*, 51, 176.
- Belokoneva, E.L., Sokolova, N.V., and Dorokhova, G.I. (1991) Crystal structure of a natural Na,Ca-scapolite: An intermediate member of the marialite-meionite series. *Soviet Physics and Crystallography*, 36, 828-830.
- Belokoneva, E.L., Sokolova, N.V., and Urusov, V.S. (1993) Scapolites—crystalline structures of marialite (Me11) and meionite (Me88)—spatial group as a function of composition. *Kristallografiya*, 38, 52-77.
- Boivin, P., and Camus, G. (1981) Igneous scapolite-bearing associations in the Chain des Puys, Massif Central (France) and Atokar (Hoggan, Algeria). *Contributions to Mineralogy and Petrology*, 77, 365-375.
- Borgstrom, L.M. (1915) Die chemische Zusammensetzung der Skapolith. *Zeitschrift für Kristallographie*, 54, 238-260.
- Burgner, R.P., Scheetz, B.E., and White, W.B. (1978) Vibrational structure of the  $S_2^-$  luminescence in scapolite. *Physics and Chemistry of Minerals*, 2, 317-324.
- Chappell, B.W., and White, A.J.R. (1968) The X-ray spectrographic determination of sulfur coordination in scapolite. *American Mineralogist*, 53, 1735-1738.
- Comodi, P., Mellini, M., and Zanazzi, P.F. (1990) Scapolites: Variation of structure with pressure and possible role in the storage of fluids. *European Journal of Mineralogy*, 2, 195-202.
- Donnay, G., Shaw, C.F., III, Butler, I.S., and O'Neil, J.R. (1978) The presence of HCl in scapolites. *Canadian Mineralogist*, 16, 341-345.
- Dunn, P.J., Nelen, J.E., and Norberg, J. (1978) On the composition of gem scapolites. *Journal of Gemmology*, 16, 4-10.
- El Shazly, E.M., and Saleeb, G.S. (1972) Scapolite-cancrinite mineral association in St. John's Island, Egypt. 24th International Geological Congress, Section 14, 192-199.
- Eugster, H.P., Protska, H.J., and Appleman, D.E. (1962) Unit-cell dimensions of natural and synthetic scapolites. *Science*, 137, 853-854.
- Evans, B.W., Shaw, D.M., and Haughton, D.R. (1969) Scapolite stoichiometry. *Contributions to Mineralogy and Petrology*, 24, 293-305.
- Gibbs, G.V., and Bloss, F.D. (1961) Indexed powder diffraction data for scapolite. *American Mineralogist*, 46, 1493-1497.
- Goldsmith, J.R., and Newton, R.C. (1977) Scapolite-plagioclase stability relations at high pressures and temperatures in the system  $NaAlSi_3O_8$ - $CaAl_2Si_2O_7$ - $CaCO_3$ - $CaSO_4$ . *American Mineralogist*, 62, 1063-1081.
- Gooding, J.L., and Muenow, D.W. (1986) Martian volatiles in shergottite EETA 79001: New evidence from oxidized sulfur and sulfur-rich aluminosilicates. *Geochimica et Cosmochimica Acta*, 50, 1049-1059.
- Gouveia, A.H., and Villarroel, H.S. (1981) Crystallographic studies of scapolites. *Revista Portuguesa de Quimica*, 23, 235-238.
- Graziani, G., and Lucchesi, S. (1982) The thermal behavior of scapolites. *American Mineralogist*, 67, 1229-1241.
- Haga, N. (1977) Cation substitution in the scapolite solid solution series. *Nippon Kessho Gakkaishi*, 19, 284-293.
- Hassan, I., and Buseck, P.R. (1988) HRTEM characterization of scapolite solid solutions. *American Mineralogist*, 73, 119-134.
- Haughton, D.R. (1971) Plagioclase-scapolite equilibrium. *Canadian Mineralogist*, 10, 854-870.
- Hazen, R.M., and Sharp, Z.D. (1988) Compressibility of sodalite and scapolite. *American Mineralogist*, 73, 1120-1122.
- Ingamells, C.O., and Gittins, J. (1967) The stoichiometry of scapolite. *Canadian Mineralogist*, 13, 214-236.
- Kuznetsova, S.V., and Skarzynsky, V.J. (1968) Scapolite from a salt caprock, Novodmitriev structure, northwestern Donetsk Basin. *Mineralogicheskiy Sbornik, L'vov*, 22, 311-315 (in Russian).
- Levien, L., and Papike, J.J. (1976) Scapolite crystal chemistry: Aluminum-silicon distributions, carbonate group disorder, and thermal expansion. *American Mineralogist*, 61, 864-877.
- Lieftink, D.J., Nijland, T.G., and Maijer, C. (1993) Cl-rich scapolite from Ødegårdens Verk, Bamble, Norway. *Norsk Geologisk Tidsskrift*, 73, 55-57.
- Lin, S.B. (1975) Crystal chemistry and stoichiometry of the scapolite group. *Acta Geologica Taiwanica*, 18, 36-46.
- Lin, S.B., and Burley, B.J. (1973a) Crystal structure of a sodium and chlorine-rich scapolite. *Acta Crystallographica*, B29, 1272-1278.
- (1973b) On the weak reflections violating body-centered symmetry in scapolites. *Tschermaks Mineralogisch-Petrologische Mitteilungen*, 20, 28-44.
- (1975) The crystal structure chemistry of an intermediate scapolite-wernerite. *Acta Crystallographica*, B31, 1806-1814.
- Llambias, E.J., Gordillo, C.E., and Bedlivy, D. (1977) Scapolite veins in

- a quartz monzodiorite stock from Los Molles, Mendoza, Argentina. *American Mineralogist*, 62, 132–135.
- Loewenstein, W. (1954) The distribution of aluminum in the tetrahedra of silicates and aluminates. *American Mineralogist*, 39, 92–96.
- Marchenko, E.I. (1961) Scapolite from the contact metasomatic formations in the granites of the middle Azov Sea. *Dopovidi Akademii Nauk Ukrainskoi RSR*, 5, 665–668.
- Moecher, D.P. (1988) Scapolite phase equilibria and carbon isotope variations in high grade rocks: Tests of the CO<sub>2</sub>-flooding hypothesis of granulite genesis. Ph.D. thesis, University of Michigan, Ann Arbor.
- Moecher, D.P., Valley, J.W., and Essene, E.J. (1994) Extraction and carbon isotope analysis of CO<sub>2</sub> from scapolite in deep crustal granulites and xenoliths. *Geochimica et Cosmochimica Acta*, 58, 959–967.
- Mykura, W., and Young, B.R. (1969) Sodic scapolite (dipyre) in the Shetland Islands. Report of the Institute of Geological Sciences, 69, 1–8.
- Orville, P.M. (1975) Stability of scapolite in the system Ab-An-NaCl-CaCO<sub>3</sub> at 4 kb and 750 °C. *Geochimica et Cosmochimica Acta*, 39, 1091–1095.
- Oterdoom, W.H., and Wenk, H.-R. (1983) Ordering and composition of scapolite: Field observations and structural interpretations. *Contributions to Mineralogy and Petrology*, 83, 330–341.
- Papike, J.J. (1964) The crystal structure and crystal chemistry of scapolite. Ph.D. thesis, University of Minnesota, Minneapolis.
- Papike, J.J., and Zoltai, T. (1965) The crystal structure of a marialite scapolite. *American Mineralogist*, 50, 641–655.
- Papike, J.J., and Stephenson, N.C. (1966) The crystal structure of mizzonite, a calcium- and carbonate-rich scapolite. *American Mineralogist*, 51, 1014–1027.
- Perizonius, R. (1966) Skapolith. *Zeitschrift der Deutschen Gesellschaft für Edelsteinkunde*, 57, 41–44.
- Peterson, R.C., Donnay, G., and LePage, Y. (1979) Sulfate disorder in scapolite. *Canadian Mineralogist*, 17, 53–61.
- Pouchou, J.L., and Pichoir, F. (1985) "PAP" (phi-rho-Z) procedure for improved quantitative microanalysis. In J.T. Armstrong, Ed., *Microbeam analysis*, p. 104–108. San Francisco Press, San Francisco, California.
- Scherillo, A. (1935) La meionite del Somma-Vesuvius. *Periodico di Mineralogia*, 6, 227–239.
- Schiebold, E., and Seumel, G. (1932) Über die Kristallostruktur von Skapolith. *Zeitschrift für Kristallographie*, 81, 100–134.
- Schwarz, H.P., and Speelman, E.L. (1965) Determination of sulfur and carbon coordination in scapolite by infra-red absorption spectrophotometry. *American Mineralogist*, 50, 656–666.
- Shannon, R.D., Oswald, R.A., and Rossman, G.R. (1992) Dielectric constants of topaz, orthoclase and scapolite and the oxide additivity rule. *Physics and Chemistry of Minerals*, 19, 166–170.
- Shaw, D.M. (1960a) The geochemistry of scapolite: I. Previous work and general mineralogy. *Journal of Petrology*, 1, 218–260.
- (1960b) The geochemistry of scapolite: II. Trace elements, petrology, and general geochemistry. *Journal of Petrology*, 1, 261–285.
- Shaw, D.M., Moxham, R.L., Filby, R.H., and Lapkowsky, W.W. (1965) The petrology of two zoned scapolite skarns. *Canadian Journal of Earth Sciences*, 2, 577–595.
- Sherriff, B.L., Grundy, H.D., and Hartman, J.S. (1987) Occupancy of T sites in the scapolite series: A multinuclear NMR study using magic-angle spinning. *Canadian Mineralogist*, 25, 717–730.
- Smetzer, K., Ottemann, J., and Krupp, H. (1976) Scapolite from central Tanzania. *Aufschluss*, 27, 341–346.
- Strunz, H., and Wilk, H. (1976) Violet scapolite of gem quality from East Africa. *Aufschluss*, 27, 389–391.
- Swayze, G.A., and Clark, R.N. (1990) Infrared spectra and crystal chemistry of scapolites: Implications for Martian mineralogy. *Journal of Geophysical Research*, 95, 14481–14495.
- Tossell, J.A. (1993) A theoretical study of the molecular basis of the Al avoidance rule and of the spectral characteristics of Al-O-Al linkages. *American Mineralogist*, 78, 911–920.
- Ulbrich, H.H. (1973a) Crystallographic data and refractive indices of scapolites. *American Mineralogist*, 58, 81–92.
- (1973b) Structural refinement of the Monte Somma scapolite, a 93% meionite. *Schweizerische Mineralogische und Petrographische Mitteilungen*, 53, 385–393.
- Wehrenberg, J.P. (1971) The infrared absorption spectra of scapolite. *American Mineralogist*, 56, 1639–1654.
- Zolotarev, A.A. (1993) Gem scapolite from the eastern Pamirs and some general constitutional features of scapolites. *Proceedings of the Russian Mineralogical Society*, 122, 90–102.
- Zwaan, P.C. (1979) More data on violet gem scapolite, probably from eastern Africa. *Journal of Gemmology*, 16, 448–451.

MANUSCRIPT RECEIVED MARCH 28, 1995

MANUSCRIPT ACCEPTED SEPTEMBER 27, 1995

## APPENDIX: MINERAL SAMPLES

PAM is a transparent, light-violet colored, gem-quality crystal from the Pamirs, Russia. Electron microprobe (EMP) compositions of several crystals and a description of the locality are given in Zolotarev (1993). No inclusions were found in our sample.

ON8 is an opaque, blue-gray scapolite from a pegmatitic skarn near Gooderham, Ontario. Bulk, wet-chemical determinations are given in Shaw (1960a, 1960b) and EMP analysis in Evans et al. (1969). Our powdered sample contains abundant analcime veining and minor calcite (this gives high bulk-sample H<sub>2</sub>O and CO<sub>2</sub> measurements). The crystal structure was refined by Papike and Zoltai (1965) with  $a = 12.060$  and  $c = 7.577$  Å, and again by Lin and Burley (1973a) with  $a = 12.059$  and  $c = 7.587$  Å.

TANZ is from a granulite near Morongoro, Tanzania. EMP composition was determined by Moecher (1988). Our powdered sample contains trace quantities of calcite and albite.

ON7 is a white, coarsely crystalline scapolite from calcareous gneiss, lot 32, Con. 17 Monmouth Township, Ontario. Bulk compositions are reported in Ingamells and Gittins (1967). Our sample contains minor analcime and potassium feldspar veining with trace plagioclase, diopside(?), and calcite. Cell parameters are  $a = 12.064$  and  $c = 7.583$  Å (Ulbrich 1973a).

CA63A is a separate of coarse-bladed, yellow-green scapolite crystals, altered along the grain margins, from a zoned skarn at Grand Calumet Township, Quebec (15 miles south of Gib Lake; Shaw et al. 1965). Wet-chemical and EMP analyses are given in Evans et al. (1969). Our sample contains traces of quartz, calcite, amphibole, and potassium feldspar (Kf<sub>85.7</sub>Cn<sub>11.9</sub>Ab<sub>2.4</sub>) and has cell parameters of  $a = 12.087$  and  $c = 7.584$  Å (Houghton 1971).

SANT is a gem-quality, transparent, light yellow crystal from Espirito Santo, Brazil (Perizonius 1966).

GL is a separate of deep blue-violet scapolite from a zoned skarn body in marble at Gib Lake, Pontiac Township, Quebec. A bulk-chemical analysis is given in Shaw et al. (1965) and an EMP analysis in Evans et al. (1969). Our sample contains albite (Ab<sub>92.8</sub>An<sub>7.2</sub>) and minor apatite and allanite. Cell parameters are  $a = 12.060$  and  $c = 7.589$  Å (Lin and Burley 1973b);  $a = 12.064$  and  $c = 7.586$  Å (Ulbrich 1973a).

ON70 is from Mpwapwa, Tanzania. Bulk-chemical and

EMP analyses are given in Evans et al. (1969). No inclusions were noted in our sample. Cell parameters are  $a = 12.063$  and  $c = 7.585$  Å (Lin and Burley 1973b);  $a = 12.081$  and  $c = 7.581$  Å (Ulbrich 1973a);  $a = 12.068$  and  $c = 7.577$  Å (Haughton 1971).

MAD is a transparent yellow gem scapolite from Madagascar. EMP analysis is given in Moecher (1988). Our sample contains trace calcite.

Q26 is from a skarn in Clapham Township, Quebec. Bulk-chemical and EMP analyses are given in Evans et al. (1969). Our sample contains minor quartz, albite, and potassium feldspar ( $Kf_{95.5}Ab_{2.8}Cn_{1.7}$ ). Cell parameters are  $a = 12.111$  and  $c = 7.578$  Å (Ulbrich 1973a);  $a = 12.099$  and  $c = 7.579$  Å (Haughton 1971).

Q13A is from a calcic gneiss, Huddersfield Township, Quebec. Bulk-chemical and EMP analyses are given in Evans et al. (1969). Our sample contains minor calcite and analcime. Cell parameters are  $a = 12.113$  and  $c = 7.576$  Å (Haughton 1971).

MIN is from a skarn near Minden, Ontario. EMP analysis is given in Moecher (1988). Our sample contains minor potassium feldspar.

ON27 is from a skarn near Olmsteadville, New York. Bulk-chemical and EMP analyses are given in Evans et al. (1969). Our sample contains trace potassium feldspar. Cell parameters are  $a = 12.142$  and  $c = 7.567$  Å (Ulbrich 1973a);  $a = 12.135$  and  $c = 7.558$  Å (Haughton 1971).

BA15 is an inclusion-free, colorless, slightly cloudy single crystal from a locality in Quebec.

BL136 is a separate of a scapolite-bearing rock from a locality in Quebec and contains abundant potassium feldspar, plagioclase, diopside, and quartz.

M18-20-1 (Brook University) is a mineral separate from

a locality in Quebec and contains abundant potassium feldspar and plagioclase.

M18-20-2 (Brook University) is from Pinks Lake, Quebec, and contains minor analcime and rare amphibole and muscovite.

BOLT is a transparent, light violet scapolite from a marble pegmatite in Bolton, Massachusetts. EMP analysis is given in Moecher (1988) and the calculated formula in Moecher et al. (1994). Our sample contains trace plagioclase and muscovite.

ON47 is from Slyudyanka, Russia; no inclusions were noted in our sample. Bulk-chemical and EMP analyses are given in Evans et al. (1969). Five bulk compositions of Slyudyanka scapolites are quoted in Shaw (1960a). Cell parameters are  $a = 12.168$  and  $c = 7.571$  Å (Lin and Burley 1973b);  $a = 12.165$  and  $c = 7.574$  Å (Ulbrich 1973a);  $a = 12.154$  and  $c = 7.575$  Å (Haughton 1971).

MONT is a colorless gemmy scapolite from vugs in an ejected marble block, Monte Somma, Italy. There are no inclusions in our sample. In some other samples the crystal margins are altered to an opaque white. Individual scapolite crystals from different vugs have slightly different compositions. Bulk compositions determined by Borgstrom (1915) and Scherillo (1935) are quoted in Shaw (1960a). EMP data are given by Evans et al. (1969), Graziani and Lucchesi (1982), Oterdoom and Wenk (1983), and Moecher (1988). The structure has been refined several times. Cell edges are  $a = 12.191$  and  $c = 7.575$  Å (Hazen and Sharp 1988);  $a = 12.194$  and  $c = 7.557$  Å (Lin and Burley 1973b);  $a = 12.189$  and  $c = 7.576$  Å (Ulbrich 1973a);  $a = 12.201$  and  $c = 7.579$  Å (Ulbrich 1973b);  $a = 12.192$  and  $c = 7.575$  and  $a = 12.200$  and  $c = 7.578$  Å (Oterdoom and Wenk 1983).